



Original Paper

Hydrocarbon expulsion model and resource potential evaluation of high-maturity marine source rocks in deep basins: Example from the Ediacaran microbial dolomite in the Sichuan Basin, China



Wen-Yang Wang ^{a,*}, Xiong-Qi Pang ^{b,c,**}, Ya-Ping Wang ^{c,f}, Zhang-Xin Chen ^d,
Chang-Rong Li ^e, Xin-Hua Ma ^g

^a State Key Laboratory of Lithospheric Evolution, Institute of Geology and Geophysics, Chinese Academy of Sciences, Beijing 100029, China

^b State Key Laboratory of Petroleum Resources and Prospecting, China University of Petroleum (Beijing), Beijing 102249, China

^c College of Geosciences, China University of Petroleum (Beijing), Beijing 102249, China

^d Chemical and Petroleum Engineering, Schulich School of Engineering, University of Calgary, Calgary T2N 1N4, Canada

^e School of Earth and Space Sciences, Peking University, Beijing 100871, China

^f Research Institute of Exploration and Development, PetroChina Southwest Oil & Gas Field Company, Chengdu, Sichuan 610041, China

^g Research Institute of Petroleum Exploration and Development (RIPED), PetroChina, Beijing 100083, China

ARTICLE INFO

Article history:

Received 13 September 2022

Received in revised form

17 November 2022

Accepted 22 November 2022

Available online 25 November 2022

Edited by Jie Hao and Teng Zhu

Keywords:

Deep petroliferous basin

Overmatured source rocks

Hydrocarbon expulsion model

Resource evaluation

Sichuan basin

ABSTRACT

Hydrocarbon expulsion features and resource potential evaluation of source rocks are crucial for the petroleum exploration. High-maturity marine source rocks have not exhibited a hydrocarbon expulsion mode owing to the lack of low-maturity source rocks in deep petroliferous basins. We considered the Ediacaran microbial dolomite in the Sichuan Basin, the largest high-maturity marine gas layer in China, to exhibit a method that quantitatively characterizes the hydrocarbon expulsion of high-maturity marine source rocks. The experiment of fluid inclusion, rock pyrolysis, and vitrinite reflectance (R_o) of 119 microbial dolomite core samples obtained from the Dengying Formation were performed. A hydrocarbon expulsion model of high-maturity source rock was established, and its resource potential was evaluated. The results showed that the Ediacaran microbial dolomite in the Sichuan Basin is a good source rock showing vast resource potential. The hydrocarbon expulsion threshold is determined to be vitrinite reflectance at 0.92%. The hydrocarbon expulsion intensities in the geologic history is high with maximum of 1.6×10^7 t/km². The Ediacaran microbial dolomite expelled approximately 1.008×10^{12} t of hydrocarbons, and the recoverable resource was 1.5×10^{12} m³. The region can be categorized into areas I, II, III, and IV, in decreasing order of hydrocarbon expulsion intensity. Areas with a higher hydrocarbon expulsion intensity have a lower drilling risk and should be prioritized for exploration in the order I > II > III > IV. Two areas, northern and central parts of Ediacaran in the Sichuan Basin, were selected as prospects which had the drilling priority in the future gas exploration. The production data of 55 drilled wells verified the high reliability of this method. This model in this study does not require low-maturity samples and can be used for evaluating high-maturity marine source rocks, which has broad applicability in deep basins worldwide.

© 2022 The Authors. Publishing services by Elsevier B.V. on behalf of KeAi Communications Co. Ltd. This is an open access article under the CC BY-NC-ND license (<http://creativecommons.org/licenses/by-nc-nd/4.0/>).

* Corresponding author.

** Corresponding author. State Key Laboratory of Petroleum Resources and Prospecting, China University of Petroleum (Beijing), Beijing 102249, China.

E-mail addresses: wywang@mail.iggcas.ac.cn (W.-Y. Wang), pangxq@cup.edu.cn (X.-Q. Pang).

1. Introduction

Carbonates are widely distributed in the petroliferous basin (Sun and Turchyn, 2014; Wang et al., 2021). Moreover, more than 40% hydrocarbon comes from carbonates layers (Xia et al., 2019). Deep marine reservoirs have substantial reserves and are considered key exploration resources for the petroleum industry globally (Hu et al., 2020; Ma et al., 2020; Wang et al., 2021). Deep oil and gas

Nomenclature

Symbols

R_o	Vitrinite reflectance (%)
TOC	Total Organic Carbon (%)
S_1	Free hydrocarbon (mg HC/g Rock)
S_2	Pyrolysis hydrocarbon (mg HC/g Rock)
I_g	Hydrocarbon generation potential (mg HC/g TOC)
I_{og}	Original hydrocarbon generation potential (mg HC/g TOC)
Roe	Hydrocarbon expulsion threshold (%)
Rol	Lower limit of hydrocarbon expulsion (%)
q_e	Hydrocarbon expulsion ratio (mg HC/g TOC)
r_e	Hydrocarbon expulsion rate (mg HC/g TOC)
I_e	Hydrocarbon expulsion intensity (t/km ²)
Q_e	Amount of hydrocarbon expulsion (t)
H	Source rock thickness (m)
ρ	Source rock density (g/cm ³)
A	Area (m ²)
Z	Depth (m)

Abbreviations

SRCA	Source–reservoir–cap assemblage
PI	Hydrocarbon accumulation probability index

drilling depth typically exceeds 4500 m which requires a large investment associated with high drilling risk (Guo et al., 2019; Geng and Wang, 2020; Chen et al., 2022a). Therefore, resource potential assessment (Athens and Caers, 2019; Wang et al., 2022) and oil exploration strategy determination before drilling is critical (Abimbola et al., 2014). Analyzing hydrocarbon expulsion characteristics is the basis for evaluating resource potential (Chen et al., 2021), which is useful for optimizing oil exploration strategies (Berntsen et al., 2018; Epelle and Gerogiorgis, 2020; Wang et al., 2020a).

Owing to the old depositional age and considerable burial depth of deep-marine highly evolved source rocks (Chen et al., 2012; Fang et al., 2017; Liu, 2019), the organic matter is in high thermal evolution stage whose vitrinite reflectance (R_o) exceeds 1.2% (Pang et al., 2022). Traditional research methods and theories associated with hydrocarbon expulsion characteristics of source rocks include natural evolution profiles, thermal simulation experiments, and basin simulation methods (Behar et al., 1992, 1995; Qiu et al., 2012; Pang et al., 2020). These methods are widely used in low-maturity source rock research areas that require low-maturity source rock samples or pyrolysis data covering the entire thermal evolution process and have limited applications in high-maturity source rock research areas (Qiu et al., 2012; Pang et al., 2020). Therefore, there is no suitable mode and method for quantitatively characterizing the hydrocarbon expulsion of high-maturity marine source rocks during geo-history, which is a challenging problem in petroleum geology (Chen and Jiang, 2015).

Many researchers have investigated the hydrocarbon expulsion of deep high-maturity marine source rocks (Rippen et al., 2013; Liu et al., 2022a, b). Several researchers have established the statistical relationship of the hydrocarbon generation of source rock samples in low-maturity and their total organic carbon (TOC) to estimate the potential of high-maturity source rocks (Jarvie et al., 2007; Chen et al., 2012, 2016; Chen and Jiang, 2015; Wu et al., 2022). Other researchers have used the kinetic parameters of kerogen–hydrocarbon generation from thermal simulation

experiments of low-maturity source rock samples to establish the evolution of hydrocarbon expulsion characteristics (Banerjee et al., 2000; Jarvie et al., 2007; Chen and Jiang, 2015; Burnham, 2019). Furthermore, others have used the pyrolysis results obtained from low-maturity source rock samples using material balance principle to simulate the hydrocarbon generation and expulsion evolution process and amount during geological history (Chen et al., 2021).

These methods use low-maturity samples from different basins, younger ages, and shallow strata to conduct comparative studies. The sedimentary environment, lithofacies, organic matter types, organic matter enrichment, and preservation conditions of source rocks in various basins or strata are different, causing variations in the kinetic parameters of kerogen–hydrocarbon generation and expulsion, resulting in high uncertainty (Katz et al., 2000; Zhang and Shuai, 2015; Makeen et al., 2015; Chen et al., 2021; Cichon-Pupienis et al., 2021). Moreover, low-maturity source rock samples rarely occur globally in deep Lower Paleozoic marine strata (Klemme and Ulmishek, 1991; Chen et al., 2012; Xia et al., 2019). Especially in the Lower Paleozoic and Precambrian marine strata of China, there are no low-mature source rocks found yet (Hanson et al., 2007; Chen et al., 2012; Xia et al., 2019; Li et al., 2021). Therefore, it is crucial to establish a model for quantitatively characterizing the high-maturity source rocks hydrocarbon expulsion during geological history without depending on immature samples.

During decades of oil and gas exploration in the Sichuan Basin, Ediacaran microbial dolomite was previously identified as a reservoir with no hydrocarbon generation during geological history (Liu et al., 2010; Xu et al., 2012). However, increased study and wells drilled for Ediacaran microbial dolomite in these years have yielded new information. These evidences, carbon and oxygen isotopes (Liu et al., 2013), co-existence of native bitumen (Liu et al., 2014), gas geochemistry (Zou et al., 2014a), indicate that the Ediacaran microbial dolomite is a potential source rock and contributes to natural gas accumulation. Because of the high maturity of Ediacaran microbial dolomite, it is challenging to characterizes their hydrocarbon generation and expulsion in geological history (Shi et al., 2020; Li et al., 2022). The breakthrough in the discovery of huge gas reserves in the Ediacaran in Sichuan Basin has attracted researchers. Thus, academic and oil industries wish to develop a good understanding of the Ediacaran microbial dolomite source rock to determine future gas exploration strategies (Zou et al., 2020).

Ediacaran microbial dolomite in the Sichuan Basin, the largest high-maturity marine gas layer in China, was considered in this study to establish a hydrocarbon expulsion model associated with high-maturity source rocks. The proved gas reserves in Ediacaran in Sichuan Basin ranked first in China and it was the first time a giant field discovered in Ediacaran globally. Combining the results obtained via experimental analysis and numerical simulation revealed that the evolution of high-maturity source rock hydrocarbon expulsion was inverted, and based on this a model was established. The resource potential of the Ediacaran microbial dolomite was assessed, and a strategy for future drilling in the Sichuan Basin was determined.

2. Geological setting

2.1. Tectonic setting

Sichuan Basin, with an area of 1.9×10^5 km², is located in central China (Hu et al., 2018; Yan et al., 2019). There are six structural units in the Sichuan Basin (Fig. 1a; Hao et al., 2008; Wang et al., 2019). Five major tectonic movements occurred in the Sichuan Basin formation and evolution corresponding to the major evolutionary stages from the Precambrian to the present (Shi et al., 2018), i.e., 1) Tongwan tectonism, with continuous subsidence during the

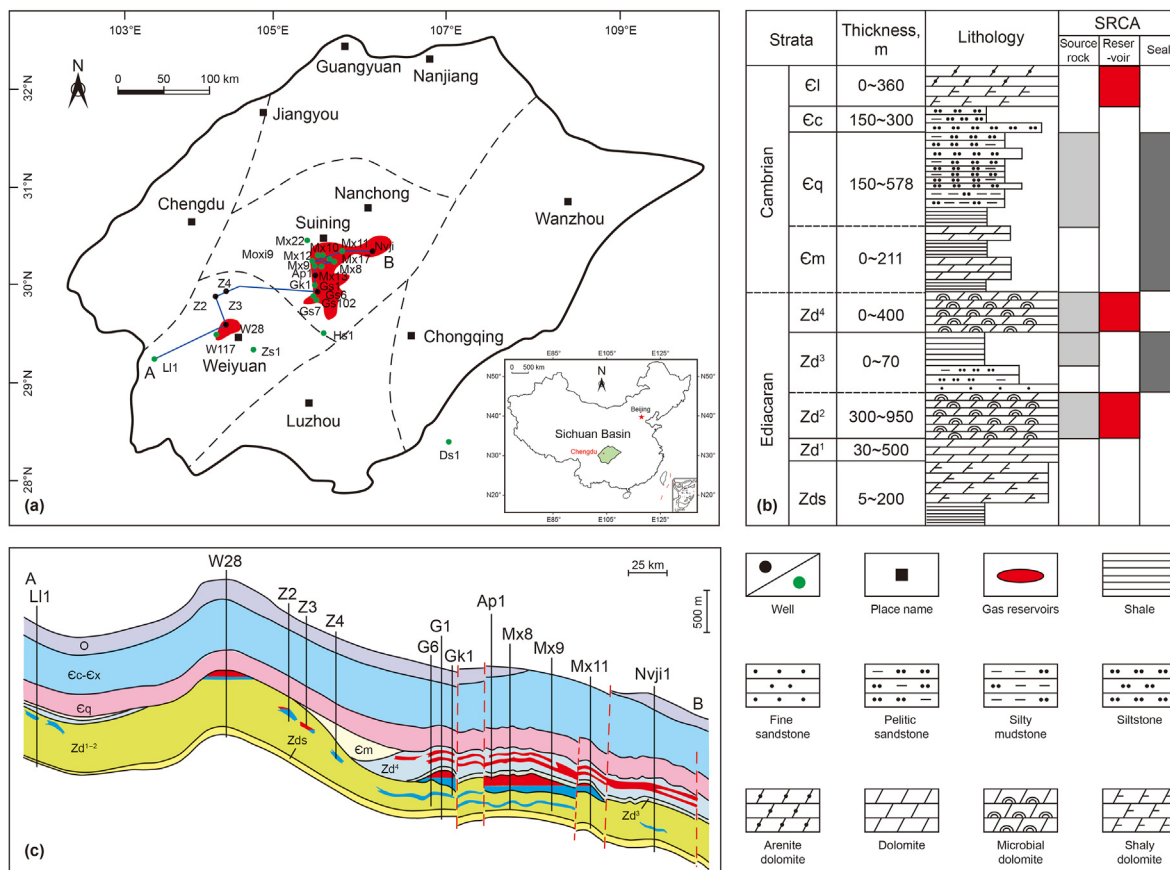


Fig. 1. (a) Location of the Sichuan Basin and sampling distribution (Wang et al., 2019). (b) Stratigraphy of the Ediacaran and Lower Paleozoic (Wang et al., 2019). (c) An important cross-section (NNE) of Ediacaran gas accumulation in Anyue gas field (Shi et al., 2018). Green wells were used for sampling. SRCA: source–reservoir–cap rock assemblage.

Ediacaran and uplift from the Late Ediacaran to the Early Cambrian, formed high quality Ediacaran reservoir (Wang et al., 2014); 2) Kwanghsian tectonism, referred to as Qilian and Wuyi–Yunkai in South China (Shi et al., 2018), the geo-history was during the Late Ordovician to the end of the Silurian, developing Leshan–Longnsvi paleouplift, the large-scale uplifts in Sichuan Basin (Chen et al., 2014); 3) Indosinian tectonism, which occurred from the Permian to the Middle Triassic and corresponded to paleouplift adjustment and reshaping (Shi et al., 2018); 4) Yanshanian and Himalayan tectonism that occurred from the Late Jurassic to the Neogene, forming an uplift in the central part (Xu et al., 2012).

2.2. Stratigraphy

The stratigraphy of the Sichuan Basin is divided into two by the upper Triassic rocks, marine carbonate strata from the Ediacaran to the lower Triassic and continental clastic sequences deposited from the lower Triassic to the present (Chen et al., 2018; Wang et al., 2019). Two sets of strata were developed in Ediacaran, including the upper Dengying and lower Doushantuo Formations (Wang et al., 2019). Ediacaran microbial dolomite mainly refers to Dengying Formation which is the focus of this study, this stratum can be further divided into four members, Zd¹–Zd⁴ (Fig. 1b). Dolomite without fungi or algae dominated Zd¹, and Zd³ consisted of mudstones with regional clastics at the bottom (Zou et al., 2014a; Shi et al., 2018). Microbial dolomite, including dolomites and thinly bedded blue-gray and ashy black dolomite mudstones, dominated Zd² and Zd⁴ (Fig. 2).

2.3. Natural gas resources

Sichuan Basin is the most abundant natural gas basin in China. Ediacaran is currently the most important gas producing layer (Yao et al., 2021; Zhu et al., 2022). In 2013, the famous gas field in China, Anyue gas field, discovered in Ediacaran in Sichuan Basin, is currently the largest natural gas field in China (Fig. 1c). By the end of 2020, the proven nature gas reserve in Ediacaran was huge and the value was $5.9 \times 10^{11} \text{ m}^3$ (Zou et al., 2020). Worldwide, there are few reports of giant gas reservoirs discovered in the Ediacaran (Zou et al., 2014b). The proved gas reserve scale in Ediacaran in Sichuan Basin ranked first in China and it is the first discovery in which natural gas can be mainly attributed to the Precambrian strata (Zou et al., 2014b; Wang et al., 2019). The rich petroleum resources in Ediacaran making Sichuan Basin as the focus and hot spot of petroleum geological studies.

3. Methods

3.1. Data and experiments

We observed and selected 19 drilling wells (e.g., Moxi 8, Gaoshi1, and Anping1) in Anyue gas field, and a total of 119 Ediacaran microbial dolomite cores were obtained. The data of TOC, R_o, and Rock-Eval were studied. Furthermore, results of previous reference were used (Shi et al., 2018). 36 core samples with captured inclusions from 9 drilling wells in Ediacaran microbial dolomite were subjected to temperature measurement analysis of fluid inclusions at 277 measuring points. Measurements were

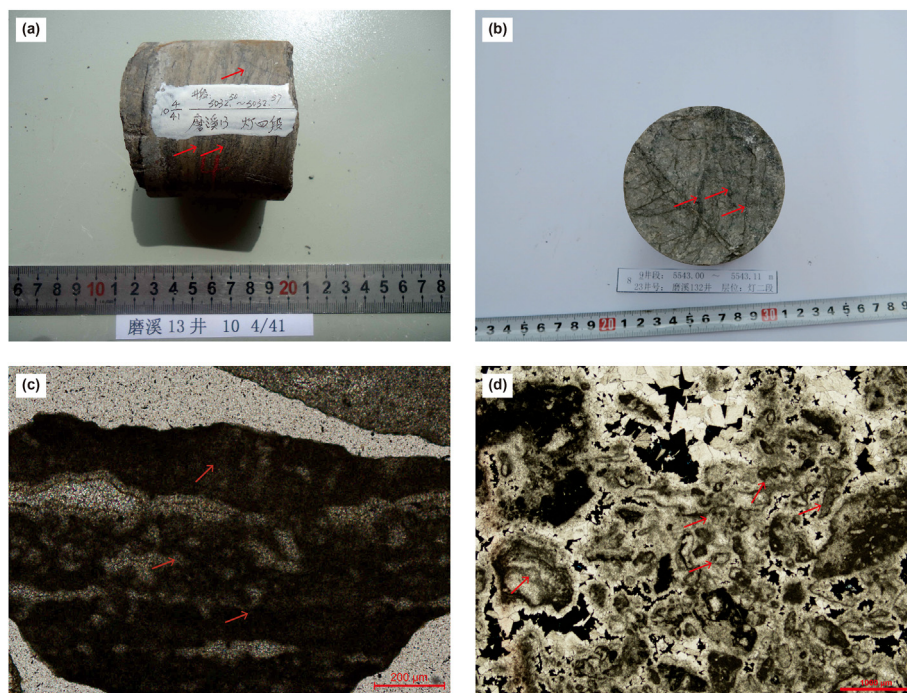


Fig. 2. Cores and microphotograph of Ediacaran microbial dolomite in Sichuan Basin (a) Well Moxi13, 5032.53 m, Zd^4 , the microbial laminite is generally dark gray in color, illustrated by the alternation of filamentous and micro-peloidal laminiae (red arrows). (b) Well Moxi132, 5043.05 m, Zd^2 , planar laminiae dominate (red arrows), represented by cm scale lamination. The alternation of dark and light dolomite intervals most likely reflects changes of organic content. (c) Well Gaoshi1, 5549 m, Zd^2 , plane-polarized light, the clotted fabric (red arrows) reflects the calcification of microbial mats and trapped micrite. (d) Well Moxi9, 5350.5 m, Zd^4 , plane-polarized light, major components include microbial peloids (red arrows) and muddy dolomiticrites.

completed by the Testing Center of the Beijing Research Institute of Uranium Geology.

The study had carried out several geochemical experiments including pyrolysis, TOC, and vitrinite reflectance analyses. Before measuring TOC, Ediacaran microbial dolomite cores need to be treated by hydrochloric to eliminate inorganic carbon. After that, the organic matter was burned and converted to CO_2 at $900\text{ }^\circ\text{C}$. All the operations were completed in combustion instrument of LECO CS-230.

Pyrolysis experiment of Ediacaran microbial dolomite cores was conducted based on Rock-Eval analyzer, and high-purity nitrogen was used as the carrier gas. Two parameters of the free hydrocarbons (S_1) and pyrolysis hydrocarbons (S_2) were obtained by the experiment. S_1 is the amount of hydrocarbon measured from rock sample in analyzer when the temperature reaches to $300\text{ }^\circ\text{C}$ and remains unchanged in 3 min. S_2 is the amount of hydrocarbon measured from rock sample in analyzer when the temperature reaches to $600\text{ }^\circ\text{C}$ and remains unchanged in 1 min. The temperature trace was nonisothermal at $25\text{ }^\circ\text{C}/\text{min}$ from $300\text{ }^\circ\text{C}$ to $600\text{ }^\circ\text{C}$. Maximum pyrolysis peak temperature (T_{max}) (Espitalié et al., 1987; Peters, 1986) was not recorded in pyrolysis experiment due to that it is meaningless for overmature samples (Yang and Horsfield, 2020; Bai et al., 2022). The vitrinite reflectance were obtained by MPV-SP microphotometer. To ensure the accuracy of the results of R_0 value, this study measured 10–20 points for each rock sample (Table S1).

The fluid inclusion experiment was conducted based on the temperature determination of fluid inclusions in minerals. The collected fluid inclusion samples were thinly sliced and polished on both sides. Fluid inclusions were observed under a microscope to obtain and categorize the expected inclusions based on their types and stages. The uniform temperature of the inclusions was measured using a LINKAM THMS600 hot and cold stage. The

experimental conditions were $20\text{ }^\circ\text{C}$ and 30% humidity under atmospheric conditions. During the temperature measurement, the operating temperature of the instrument was -196 to $600\text{ }^\circ\text{C}$ ($\pm 0.1\text{ }^\circ\text{C}$), the temperature trace was nonisothermal at $10\text{ }^\circ\text{C}/\text{min}$ and $1\text{ }^\circ\text{C}/\text{min}$ near the phase transition temperature.

3.2. Hydrocarbon expulsion conceptual model

The process of hydrocarbon generation and expulsion follows material balance (Jiang et al., 2016; Peng et al., 2016), i.e., the total expelled hydrocarbon from source rock in the geo-history and residual hydrocarbon is equal to the amount of total generated hydrocarbon in the geo-history. $(S_1+S_2)/\text{TOC}$ is a generation potential index (I_g ; Zhou and Pang, 2002) reflecting the hydrocarbon generation potential. I_g decreases when source rock beginning to expel hydrocarbon with an increase of the depth or maturity. The geological condition (depth or maturity) when I_g of source rock beginning decreasing is corresponding to threshold of source rock expelling hydrocarbon, called hydrocarbon expulsion threshold (Roe, Pang et al., 2005). I_g of source rock corresponding to Roe is the original hydrocarbon generation potential (I_{og} , Jiang et al., 2016). I_{og} is the hydrocarbon generation capacity before expulsion (Fig. 3a).

The difference between I_{og} and I_g (Eq. (1)) is an index indicating the hydrocarbons released per unit of organic carbon below Roe, called hydrocarbon expulsion ratio (q_e) (Fig. 3b). The rate of change of I_{og} of source rock with the degree of maturity, called hydrocarbon expulsion rate (r_e), is an index indicating the rate at which the source rocks expel hydrocarbons, which increases continuously with increasing burial depth and gradually decreases to the minimum until it reaches its peak (Pang et al., 2005) (Fig. 3c). The r_e decrease to the minimum corresponds to the geological condition of the lower limit of hydrocarbon expulsion (RoI), where the source rocks no longer expel hydrocarbons (Pang et al., 2020). r_e is

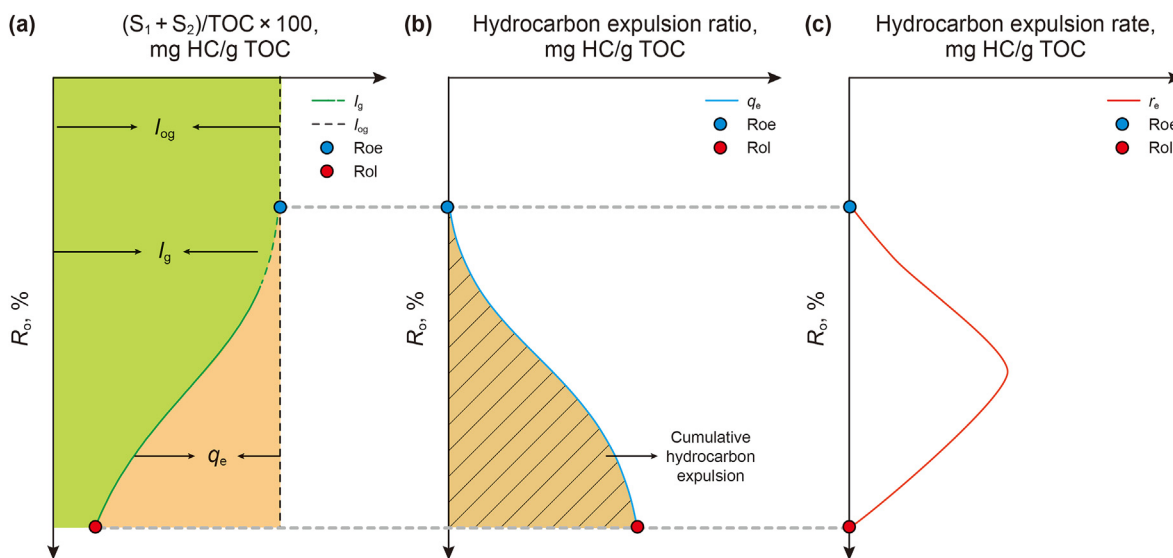


Fig. 3. Conceptual model of hydrocarbon expulsion of high-maturity source rocks.

calculated using Eq. (2) as follows:

$$q_e(R_o) = I_{og}(R_o) - I_g(R_o) \tag{1}$$

$$r_e(R_o) = \frac{dq_e}{dR_o} \tag{2}$$

However, as the measured TOC represents residual organic carbon (Espitalié et al., 1987), the original TOC should be restored based on TOC measured using Eqs. (3) and (4) and the mass balance principle.

$$TOC_o = TOC \times k \tag{3}$$

$$k = \left(1 - 0.83 \times \frac{I_g}{1000}\right) / \left(1 - 0.83 \times \frac{I_{og}}{1000}\right) \tag{4}$$

Hydrocarbon expulsion intensity was obtained using Eq. (5), and hydrocarbon expulsion amount was obtained using Eq. (6):

$$I_e = \int_{R_o^t}^{R_o} 10^{-3} \times q_e(R_o) \times H \times \rho \times TOC_o(R_o) \times d(R_o) \tag{5}$$

$$Q_e = \int_{R_o^t}^{R_o} 10^{-3} \times q_e(R_o) \times H \times A \times \rho \times TOC_o(R_o) \times d(R_o) \tag{6}$$

where q_e represents the hydrocarbon expulsion ratio (mg HC/g TOC), H represents the thickness of the source rock (m), ρ represents the density (g/cm³), A represents the area (m²), TOC_o represents the original TOC (%), I_e represents the hydrocarbon expulsion intensity (10⁴ t/km²), and Q_e represents the amount of hydrocarbon expulsion (10⁸ t).

Vitrinite is not widely developed in the Ediacaran (Chen et al., 2021). In this study, pyrobitumen reflectance was measured and the equivalent vitrinite reflectance was obtained based on equation proposed by Jacob (1985). Thermal and burial history of basin is a good data to determine the relationship between source rock thermal maturity and depth (Liu et al., 2021, 2022a,b; Li et al., 2021). Based on the burial and thermal histories of source rock of Ediacaran Dengying Formation (details showed in Fig. 7, Zou al.,

2014a), the vitrinite reflectance of Ediacaran microbial dolomite source rock in the Sichuan Basin was obtained using Eq. (7):

$$R_o = 0.31 \times \exp(0.0004 \times Z) \tag{7}$$

where R_o represents the vitrinite reflectance of kerogen in the source rock (%), Z represents the depth of source rock (m).

3.3. Workflow

Four steps are required to establish a model of hydrocarbon expulsion of source rocks in high-maturity and evaluate their resource potential. First, the critical conditions associated with hydrocarbon expulsion from highly evolved source rocks were determined, the I_{og} of source rocks was inverted, and a hydrocarbon expulsion model for highly evolved source rocks was established. The method for determining the critical conditions associated with hydrocarbon expulsion (Roe) was as follows. We obtained a homogeneous temperature distribution map of fluid inclusions based on the experiment and determined the main peak value of the homogeneous temperature of the first-phase inclusions using the homogeneous temperature distribution map. Many isotherms were present in the profile of the sedimentary burial history and thermal evolution of the well. The main peak value of the homogeneous temperature of the first-phase inclusions corresponded to an isotherm, and the minimum R_o for this isotherm is the critical condition for Roe.

The hydrocarbon expulsion evolution profile inverted the I_{og} of the source rock. The I_g envelope was drawn on the evolution profile of $(S_1+S_2)/TOC$, and the mathematical relationship between R_o and I_g was obtained by Matlab software, Eq. (8).

$$I_g = \frac{a}{1 + e^{(b \times R_o + c)}} + d \tag{8}$$

where I_g is the hydrocarbon generation potential (mg HC/g TOC), and a , b , c , and d are constants.

Based on the Roe and Eq. (8), the I_{og} was obtained as follows:

$$I_{og} = \frac{a}{1 + e^{(b \times Roe + c)}} + d \tag{9}$$

where I_{og} is the original hydrocarbon generation potential (mg HC/

g TOC), Roe is the critical condition of hydrocarbon expulsion (%), and a , b , c , and d are the constants obtained in Eq. (8).

Based on Roe and I_{og} , a hydrocarbon expulsion model for high-maturity marine source rocks can be established.

Then the hydrocarbon expulsion ratio (q_e) and rate (r_e) of the source rock are determined. Based on the established hydrocarbon expulsion model, two parameters of q_e and r_e can be calculated based on Eqs. (1) and (2), respectively. After that, the lower limit of hydrocarbon expulsion of the source rock (R_{ol}) was determined when r_e was minimized.

Next, the hydrocarbon expulsion intensity (I_e) and expulsion amount (Q_e) are determined. Based on the established hydrocarbon expulsion model, I_e and Q_e were obtained using Eqs. (5) and (6), respectively.

Finally, we evaluated the resource potential and determined oil exploration strategies for drilling. The amount of hydrocarbon expulsion is the basis for evaluating the resource potential. When the hydrocarbon expulsion is larger, the resource potential is as well. The hydrocarbon expulsion intensity can be used directly to predict favorable oil and gas drilling areas. Areas with higher hydrocarbon expulsion intensity have higher drilling success and lower drilling risk and should be prioritized for drilling in future explorations.

4. Results

4.1. Bulk geochemical parameters

Bulk geochemical analysis based on TOC and Rock-eval data is essential for source rock evaluation (Liu et al., 2019). The measured TOC for 119 microbial dolomite samples ranged from 0.04% to 6.33% with an average of 1.41%. The S_1+S_2 value of the microbial dolomite ranged from 0.03 to 4.96 mg/g with an average value of 0.81 mg/g. The TOC value of 64% of the samples was higher than 1%. According to the TOC versus S_1+S_2 diagrams (Fig. 4a) and the TOC histograms (Fig. 4b), most of the microbial dolomites are good source rocks. The cross-plot of dimensionless S_2 and TOC shows that the Ediacaran microbial dolomite is type I kerogen (Fig. 4c).

4.2. Critical conditions of hydrocarbon expulsion and original hydrocarbon generation potential of Ediacaran microbial dolomite

(1) Inclusion development stage and uniform temperature

Based on the inclusions identified under a microscope and different inclusion development locations, three main inclusion stages occurred in the Ediacaran Dengying Formation, i.e., the first, second, and third stage inclusions developed during early dolomite grain formation (Fig. 5a and b), late dolomite and quartz filling (Fig. 5c and d), and late dolomite and quartz microfracture

formation (Fig. 5e and f), respectively. The results of this study are consistent with those reported by Zhou et al. (2015), who showed that three main stages of inclusion occurred in the Ediacaran Dengying Formation. The differences in the formation order of the inclusions during the three periods yielded different main temperature peaks (Fig. 6). The peak temperature of the inclusions in the first-stage dolomite grains was low, i.e., 120–130 °C, whereas that in the second-stage dolomite or quartz filling was 140–150 °C. The peak temperature of the inclusions in the third-stage dolomite or quartz microcracks was relatively high, i.e., 150–160 °C.

(2) Critical conditions for hydrocarbon expulsion

The peak temperature of the first-stage inclusion homogenization was between 120 °C and 130 °C. For quantitative characterization, the median value was 125 °C (the main peak of the first-stage inclusion homogenization temperature), representing the beginning of Ediacaran microbial dolomite source rocks expelling hydrocarbon at this palaeogeotemperature. Fig. 7 is the sedimentary burial history and thermal evolution profile, Roe of the Ediacaran microbial dolomite source rocks was inverted. At 125 °C, as shown in Fig. 7, the minimum R_o was 0.92% (Roe = 0.92%), indicating that when the maturity of the Ediacaran microbial dolomite exceeded 0.92%, they expelled hydrocarbons.

(3) Original hydrocarbon generation potential

The evolution profile of I_g of Ediacaran microbial dolomite source rocks based on the experimental results of rock pyrolysis is shown in Fig. 8a. The I_g envelope was drawn on the evolution profile, and the mathematical relationship between R_o and I_g was obtained using MATLAB as follows:

$$I_g = \frac{699.6}{1 + e^{(3.6R_o - 7.1)}} + 61.4 \quad (10)$$

In the evolution profile, the hydrocarbon generation potential corresponding to Roe was the I_{og} of the source rock. Using Eq. (10), the I_{og} of Ediacaran microbial dolomite source rocks of Sichuan Basin is 756 mg HC/g TOC.

4.3. Hydrocarbon expulsion model of Ediacaran microbial dolomite

The hydrocarbon expulsion model of Ediacaran microbial dolomite was established based on the pyrolysis data, hydrocarbon expulsion threshold, and I_{og} of Ediacaran microbial dolomite source rocks of Sichuan Basin. The model shows that Ediacaran microbial dolomite enters the threshold when R_o is 0.92% and I_g decreases, i.e., Roe of Ediacaran microbial dolomite is 0.92% (Fig. 8a). Below 0.92%, the r_e of Ediacaran microbial dolomite increased (Fig. 8b). When R_o was 2.1%, the r_e was to the top (Fig. 8c). When R_o was 3.5%,

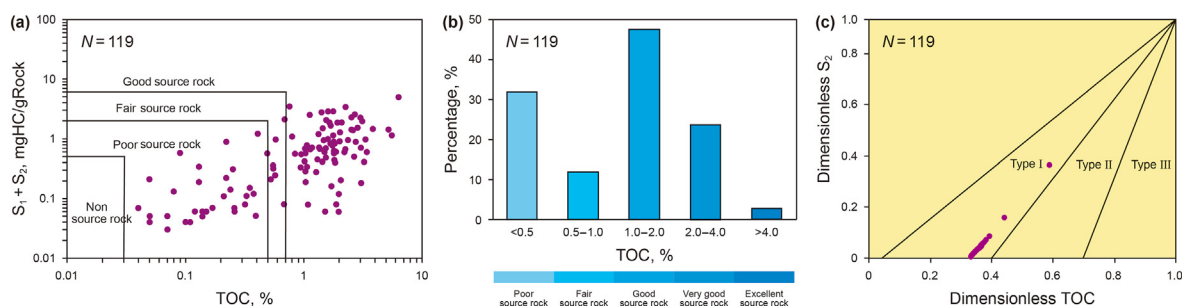


Fig. 4. Bulk geochemical analysis of Ediacaran microbial dolomite in Sichuan Basin. (a) (S_1+S_2) versus TOC. (b) TOC histograms. (c) Dimensionless S_2 vs. TOC plot.

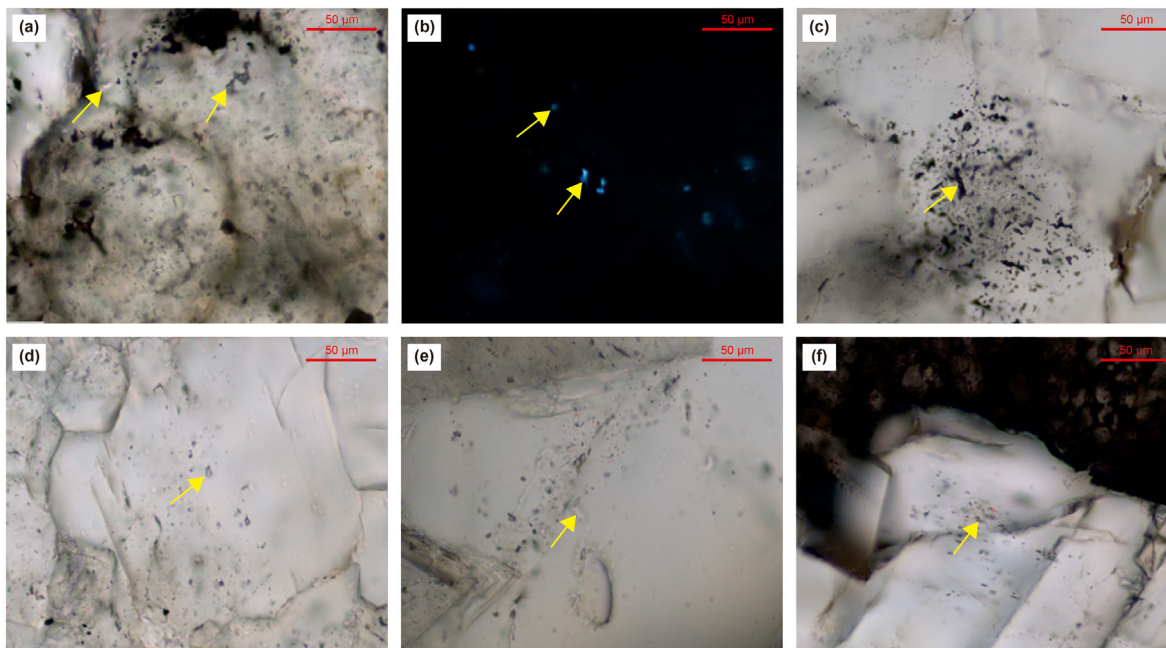


Fig. 5. The fluid inclusion identification and microscopic features in the Ediacaran Dengying Formation. (a) Well Gaoshi 102, 5156.4 m, single polarized light. The inclusions are distributed along the microcracks of microbial dolomite grains and pore fillings. Transparent and colorless gas-liquid hydrocarbon and dark-gray natural gas inclusions exhibiting blue fluorescence are present. (b) Well Gaoshi 102, 5156.4 m, single polarized light. The ultraviolet (UV)-excited fluorescence photo shows a distribution along the microcracks of the dolomite grains and pore fillings. Transparent and colorless gas-liquid hydrocarbon inclusions possessing dark-blue fluorescence and natural gas inclusions are present. (c) Well Gaoshi 102, 5033.3 m, single polarized light. Microbial dolomite pores and quartz fillings are distributed in clusters with dark-brown liquid hydrocarbon inclusions. (d) Well Wei 77, 3115.5 m, single polarized light. Fine-grained dolomite and cave dolomite fillings are clustered. Colorless-to-gray hydrocarbons containing brine and dark-gray natural gas inclusions are present. (e) Well Gaoke 1, 5028.4 m, single polarized light. The distribution is along the microcracks of the quartz fillings of the algal-stacked dolomite cave, with colorless-to-gray hydrocarbons containing brine and dark-gray natural gas inclusions. (f) Well Anping 1, 5057.2 m, single polarized light. The distribution is along the microcracks of the quartz fillings in the dolomite cavity, with colorless-to-gray hydrocarbons.

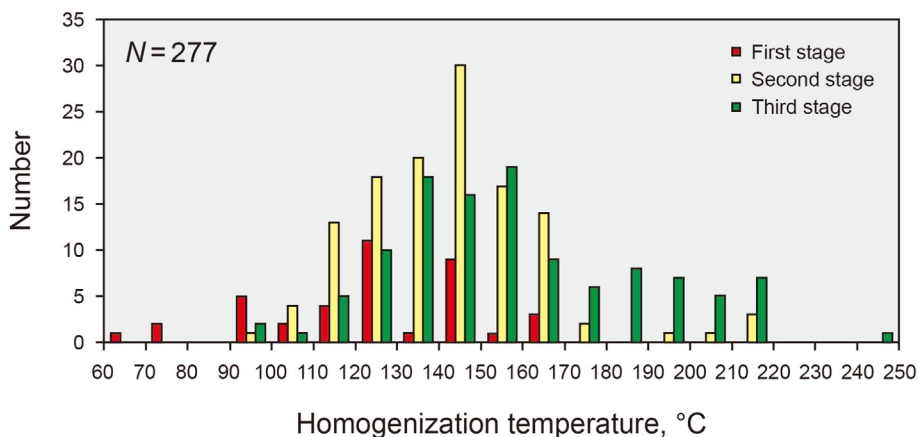


Fig. 6. Distribution and features of homogenization temperature of fluid inclusions in the Ediacaran Dengying Formation.

r_e decreased to the minimum and remained unchanged, indicating that Ediacaran microbial dolomite source rocks reached to RoI, and the process ended.

4.4. Hydrocarbon expulsion intensities and amounts of Ediacaran microbial dolomite source rocks

By the hydrocarbon expulsion model of Ediacaran microbial dolomite source rocks of Sichuan Basin and burial and thermal evolution histories, the hydrocarbon expulsion characteristics of Ediacaran microbial dolomite source rocks in the geo-history was quantitatively characterized. The hydrocarbon expulsion intensities

and amounts of Ediacaran microbial dolomite source rocks of Sichuan Basin corresponding to different geological periods were calculated using Eqs. (5) and (6), respectively.

The Ediacaran microbial dolomite source rocks have undergone multiple burial and uplift evolutionary processes. During the Silurian, R_o was 0.92%, reaching Ro_e, and the dolomite source rocks expelled hydrocarbon. However, during the Silurian, the Caledonian movement (Ma et al., 2019) uplifted and eroded the Sichuan Basin until 140 Ma, after which microbial dolomite hydrocarbon expulsion ceased. Few hydrocarbon expulsions occurred during the Silurian period. Fig. 9 depicts the hydrocarbon expulsion intensity of microbial dolomites at the end of the Silurian. There was one

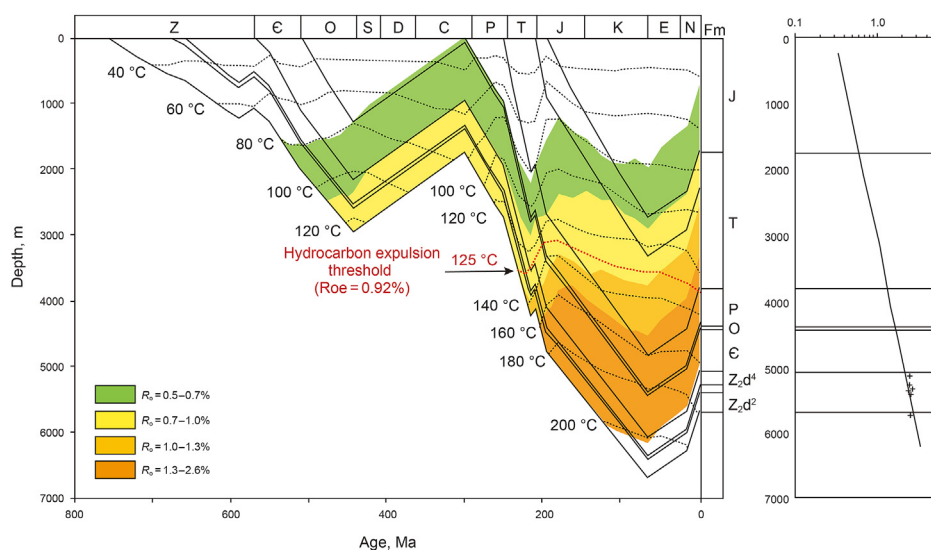


Fig. 7. Thermal evolution and burial history of the Ediacaran microbial dolomite source rocks, Well Moxi 8 in Sichuan Basin (Zou et al., 2014a).

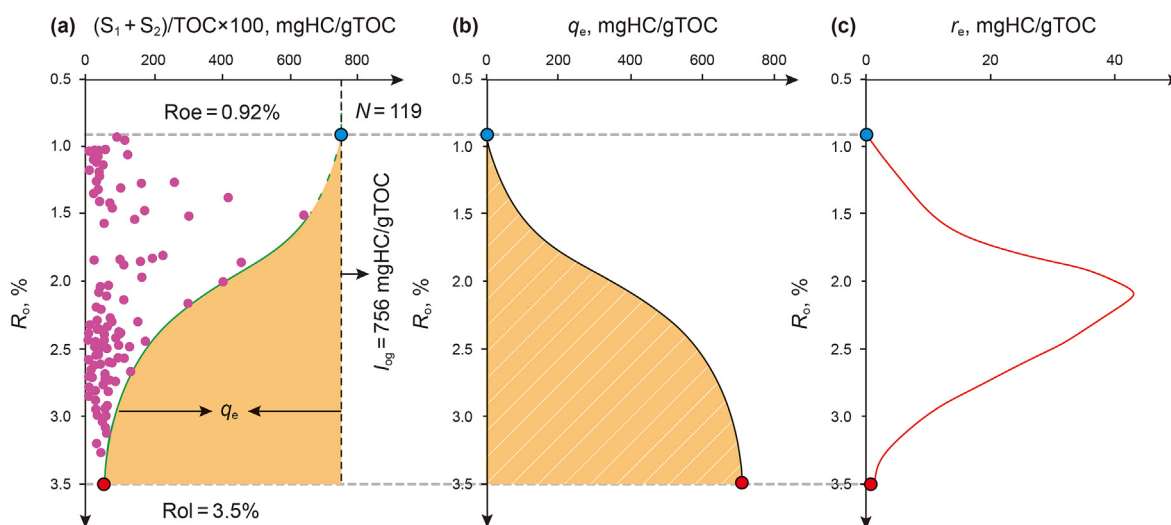


Fig. 8. The quantitative model of the hydrocarbon expulsion of the Ediacaran microbial dolomite source rocks in Sichuan Basin. Green circle is the hydrocarbon expulsion threshold (Roe) and red circle is the lower limit of hydrocarbon expulsion (Rol).

center with intensity of 5.0×10^5 t/km² (Fig. 9a). The total expelled amount of the Ediacaran microbial dolomite source rocks at the end of the Silurian was 7.76×10^9 t. During the Permian, the Ediacaran Dengying Formation underwent rapid subsidence of 60 m/Ma, and the microbial dolomite source rocks re-expelled hydrocarbons. In the Triassic, the microbial dolomite hydrocarbon expulsion range was relatively wide. There was one center with intensity of 1.0×10^7 t/km² (Fig. 9b). The total expulsion amount of Ediacaran microbial dolomite between the end of the Silurian and Triassic was 5.7752×10^{11} t. At the end of the Jurassic, there was one center with intensity of 1.6×10^7 t/km² (Fig. 9c), and the total expulsion amount between Triassic and the end of the Jurassic was 3.9584×10^{11} t. The Himalayan movement (Ma et al., 2019) in the Late Cretaceous caused considerable uplift in the basin, and hydrocarbon expulsion ceased. Therefore, the hydrocarbon expulsion intensities have been consistent since the end of the Cretaceous. There was one center (Fig. 9d), and the total expulsion amounts between the end of the Jurassic and the end of the Cretaceous was 2.716×10^{10} t. Fig. 10 and Table S2 show the details of hydrocarbon expulsion amounts of the

Ediacaran microbial dolomite in Sichuan Basin during different periods, as well as the cumulative amounts.

5. Discussion

The hydrocarbon expulsion centers control favorable accumulation areas of hydrocarbons (Peters et al., 2015; Hu et al., 2021). This section investigates the Ediacaran microbial dolomite accumulation period, resource potential, and hydrocarbon expulsion center that control areas favorable for hydrocarbon exploration.

5.1. Hydrocarbon accumulation stage

This study analyzed the Ediacaran microbial dolomite accumulation period based on the hydrocarbon expulsion in the geohistory. The primary hydrocarbon expulsion period in a hydrocarbon source can be considered the accumulation stage of hydrocarbon. Based on the histogram of microbial dolomite hydrocarbon expulsion in different periods (Fig. 10), there were two main

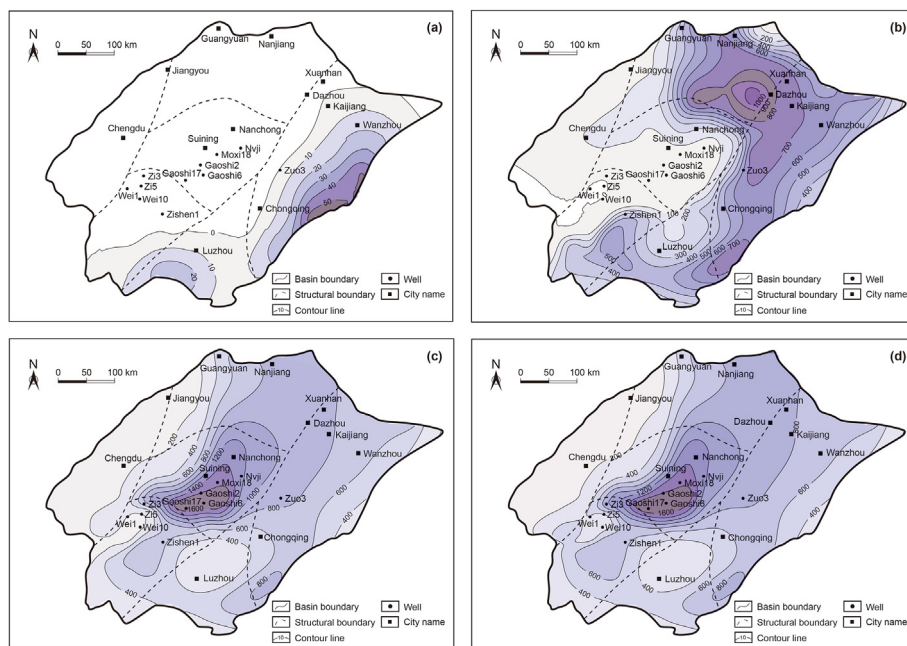


Fig. 9. Hydrocarbon expulsion intensity of Ediacaran microbial dolomite. (a) And of the Silurian; (b) Triassic; (c) And of the Jurassic; (d) And of the Cretaceous. The unit of the intensity contour line is 10^4 t/km².

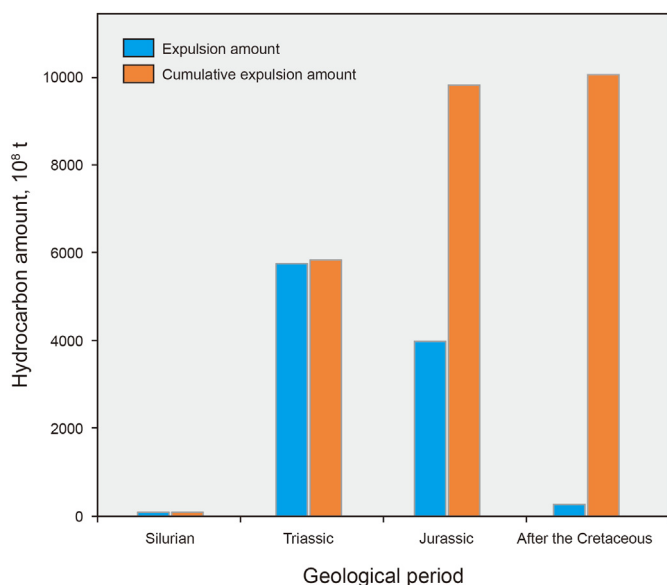


Fig. 10. Hydrocarbon expulsion amounts of Ediacaran microbial dolomite in Sichuan Basin in geo-history.

hydrocarbon expulsion events in the geological history, which occurred in the Triassic and Jurassic. There are two periods with relatively low hydrocarbon expulsion, which can be ignored.

5.2. Oil and gas prospects and future exploration strategies in Sichuan Basin

The resource potential and favorable areas of the Dengying Formation can be evaluated using hydrocarbon expulsion amounts and intensities to determine oil exploration strategies for the future gas exploration in the Sichuan Basin. Gas exploration of the Dengying Formation has shown significant improvement.

The oil test data of Well Gaoshi 1 displayed an enormous resource potential of 1.4×10^6 m³/day. The gas source of the Dengying Formation was primarily microbial dolomite (Zou et al., 2014a), which has good hydrocarbon generation potential. As it was affected by the strong weathering crustal karstification of the Tongwan movement, dissolution pores dominated the microbial dolomite reservoir space in the Dengying Formation. In addition, intergranular pores, intercrystalline pores, and karst caves have developed (Zou et al., 2014b; Wei et al., 2020). The mudstones of the Qiongzhusi Formation were widely distributed and were 80–150 m thick in the Gaoshiti–Moxi area, providing good cover for the Dengying Formation (Wei et al., 2020). Therefore, the Dengying Formation experienced favorable accumulation conditions (Ma et al., 2019).

Based on the hydrocarbon expulsion model, the microbial dolomite of the Dengying Formation expelled approximately 1.008×10^{12} t of hydrocarbons (Table S2). Considering that this formation is a source rock and a reservoir with a deep burial depth, an aggregation coefficient of 1% (Zou et al., 2014a) was used to determine the resources of the Dengying Formation from microbial dolomite. The amount was 1.008×10^{10} t (1.26×10^{13} m³), exhibiting excellent exploration potential. Available resources only accounted for a portion of the accumulated resources and are defined as those other than dead oil and gas confined in the reservoirs (Theloy and Sonnenberg, 2013; Zou et al., 2014b). Recoverable resources can eventually be produced under current technical conditions and account for a portion of the available resources. Based on the results of several scholars and institutions, the average available ratio of tight gas is 32.4% (USGS, 2009; Gao and Li, 2015), and the average tight gas recovery ratio is 37.0% (USGS, 2009; Zou et al., 2012; C&C, 2015). Thus, the recoverable resource amount in the Sichuan Basin is estimated to be 1.5×10^{12} m³ from the microbial dolomite source rocks of the Dengying Formation. Based on the current natural gas production rate of 35.4 billion cubic meters per year (2021 production, Zhang, 2022), stable production can be ensured for 43 years, indicating an enormous potential for future production.

Source rocks, particularly hydrocarbon expulsion centers, control the distribution range of hydrocarbon resources (Jiang et al., 2016; Wu et al., 2022; Chen et al., 2022b). Wang et al. (2019) reported that hydrocarbon expulsion intensity has dominated oil and gas accumulation. For higher hydrocarbon expulsion intensity, the hydrocarbon accumulation probability is higher and drilling risk is lower (Fig. 11a and b). To quantitatively predict favorable oil and gas exploration areas and scientifically determine oil and gas exploration strategies, this study proposed a hydrocarbon accumulation probability index (PI) that reflected the probability of hydrocarbon accumulation. PI ranged from 0 to 1. Furthermore, when PI is greater, the probability of hydrocarbon accumulation is greater, the success rate of drilling is higher.

The hydrocarbon accumulation probability index is relative. A target zone with $PI = 1$ does not mean that the petroleum drilling success rate is 100%. The zone with bigger PI means better choice compared to others. Based on the PI , they were divided into areas I ($0.75 < PI \leq 1$), II ($0.5 < PI \leq 0.75$), III ($0.25 < PI \leq 0.5$), and IV ($0 \leq PI \leq 0.25$). The descending order of PI for these areas was I, II, III, and IV; therefore, the drilling priority was $I > II > III > IV$.

The Triassic and Jurassic were the two major accumulation periods for the Dengying Formation (Fig. 10). For the hydrocarbon expulsion intensity distribution in the two main expulsion periods (Fig. 9b and c), the hydrocarbon expulsion intensity was normalized. The PI at the highest hydrocarbon expulsion intensity was defined as 1, and in other areas, it was the ratio of the hydrocarbon expulsion intensity at the location to the highest expulsion intensity. The accumulation index of all areas on the plane was distributed between 0 and 1. Therefore, Triassic and Jurassic accumulation period PI distribution maps were obtained and divided into areas I, II, III, and IV. Because the current hydrocarbon accumulation area is the sum of the accumulation areas for the main accumulation periods throughout geological history (Wang et al., 2019), the current hydrocarbon accumulation areas and the sum of hydrocarbon accumulation areas during the Triassic and Jurassic were obtained (Fig. 11c). As shown in Fig. 11c, to limit the drilling risk, area I was primarily distributed in the northern and central areas of the Sichuan Basin, which were selected as priority areas for future exploration of the Ediacaran Dengying Formation.

5.3. Reliability verification

In this study, the succeed drilling wells are industrial gas wells,

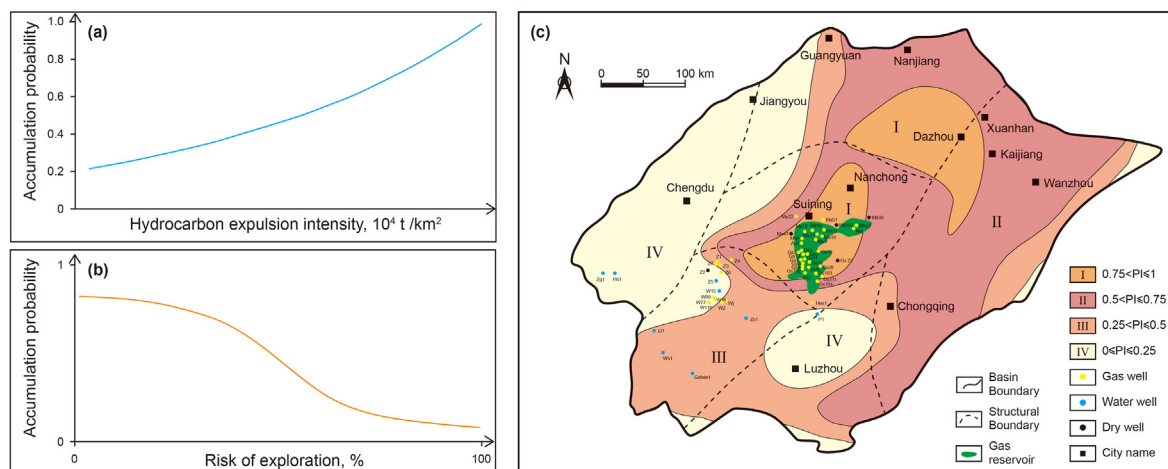


Fig. 11. (a) The relationship between hydrocarbon expulsion intensity and PI (modified from Wang et al., 2019). (b) The relationship between PI and drilling risk (modified from Wang et al., 2020a). (c) The distribution of PI of Ediacaran Dengying Formation of Sichuan Basin and drilling priority. PI is the hydrocarbon accumulation probability index.

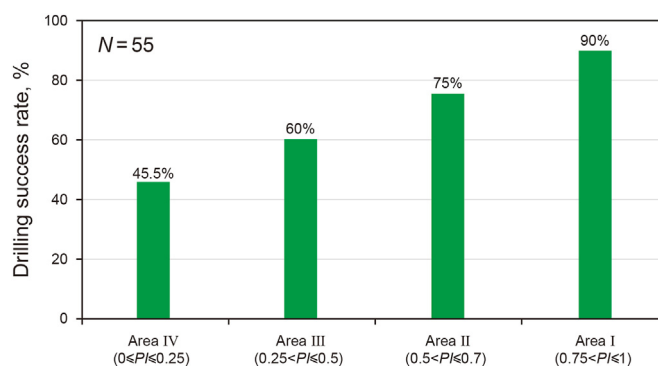


Fig. 12. The drilling success rate in areas with different hydrocarbon accumulation indexes (PI) in the Dengying Formation.

and the failed wells refer to water wells and dry wells (Wang et al., 2019). The production results obtained from 55 drilling wells in the Ediacaran Dengying Formation showed that the drilling success rates in areas I, II, III, and IV were 90%, 75%, 60%, and 45.5%, respectively (Fig. 12), as shown in Table S3. The results exhibited a positive correlation between PI and drilling success rate. A higher PI value correlates to a higher drilling success rate, verifying the reliability of the evaluation of favorable oil and gas exploration areas based on PI .

5.4. Improvement on the traditional hydrocarbon expulsion model

The traditional hydrocarbon expulsion model, based on the mass balance, using Rock-Eval data covering low maturity and high maturity to quantify hydrocarbon expulsion and the petroleum resource potential (Thompson and Dembicki, 1986; Pang et al., 2005; Varma et al., 2015; Wang et al., 2020b). This method has been widely employed in global middle and shallow petroliferous basins with low-maturity source rocks (Peng et al., 2016; Jiang et al., 2016; Wu et al., 2022; Chen et al., 2022b). However, the traditional method relies on low-maturity source rocks, which have limited applications in high-maturity source rock research areas of deep petroliferous basins (Chen et al., 2022b). Through a combination of experimental analysis and numerical simulation, the evolution process of hydrocarbon expulsion of high-maturity source rocks was inverted, and a hydrocarbon expulsion model was established

in this study. This model does not require low maturity samples and is suitable for evaluating high maturity marine source rocks with broad applicability in deep petroliferous basins.

6. Conclusions

The hydrocarbon expulsion model established in this study is suitable for evaluating high-maturity marine source rocks, solving the problem that traditional evaluation methods depend on low-maturity samples and are limited in application to the high-maturity source rock areas of deep petroliferous basins. Based on this model, hydrocarbon expulsion from high-maturity source rock can be quantitatively evaluated, and the resource potential of the study area can be predicted. Areas with a higher hydrocarbon expulsion intensity have a lower drilling risk and should be prioritized for drilling in the order of I > II > III > IV.

The Ediacaran microbial dolomite in the Sichuan Basin is a good source rock and has a vast resource potential. The amount of hydrocarbon expulsion was 1.008 trillion tons, and the recoverable resource was 1.5 trillion m³, guaranteeing stable production for 43 years. The northern and central areas of the Sichuan Basin were selected as prospects and two priority areas for future exploration of the Ediacaran Dengying Formation.

Declaration of competing interest

The authors declare that they have no known competing financial interests or personal relationships that could have appeared to influence the work reported in this paper.

Acknowledgments

This work was supported by the Open Fund Project of State Key Laboratory of Lithospheric Evolution [SKL-K202103]. We appreciate the support of the Exploration and Development Research Institute of PetroChina Southwest Oil & Gas Field. We would like to thank Prof. Zhu Rixiang from the Institute of Geology and Geophysics, Chinese Academy of Sciences, for his important suggestions on the establishment of the hydrocarbon expulsion model in this study.

Appendix A. Supplementary data

Supplementary data related to this article can be found at <https://doi.org/10.1016/j.petsci.2022.11.018>.

References

- Abimbola, M., Khan, F., Khakzad, N., 2014. Dynamic safety risk analysis of offshore drilling. *J. Loss Prev. Process. Ind.* 30, 74–85. <https://doi.org/10.1016/j.jlp.2014.05.002>.
- Athens, N.D., Caers, J.K., 2019. A Monte Carlo-based framework for assessing the value of information and development risk in geothermal exploration. *Appl. Energy* 256, 113932. <https://doi.org/10.1016/j.apenergy.2019.113932>.
- Bai, L.H., Liu, B., Du, Y.J., et al., 2022. Distribution characteristics and oil mobility thresholds in lacustrine shale reservoir: insights from N₂ adsorption experiments on samples prior to and following hydrocarbon extraction. *Petrol. Sci.* 19 (2), 486–497. <https://doi.org/10.1016/j.petsci.2021.10.018>.
- Banerjee, A., Jha, M., Mittal, A.K., et al., 2000. The effective source rocks in the north Cambay Basin, India. *Mar. Petrol. Geol.* 17 (10), 1111–1129. [https://doi.org/10.1016/S0264-8172\(00\)00049-0](https://doi.org/10.1016/S0264-8172(00)00049-0).
- Behar, F., Kressmann, S., Rudkiewicz, J.L., et al., 1992. Experimental simulation in a confined system and kinetic modelling of kerogen and oil cracking. *Org. Geochem.* 19 (1–3), 173–189. [https://doi.org/10.1016/0146-6380\(92\)90035-V](https://doi.org/10.1016/0146-6380(92)90035-V).
- Behar, F., Vandenbroucke, M., Teermann, S.C., et al., 1995. Experimental simulation of gas generation from coals and a marine kerogen. *Chem. Geol.* 126 (3–4), 247–260. [https://doi.org/10.1016/0009-2541\(95\)00121-2](https://doi.org/10.1016/0009-2541(95)00121-2).
- Berntsen, M., Bøe, K.S., Jordal, T., et al., 2018. Determinants of oil and gas investments on the Norwegian Continental Shelf. *Energy* 148, 904–914. <https://doi.org/10.1016/j.energy.2018.01.147>.
- Burnham, A.K., 2019. Kinetic models of vitrinite, kerogen, and bitumen reflectance. *Org. Geochem.* 131, 50–59. <https://doi.org/10.1016/j.orggeochem.2019.03.007>.
- C&C, 2015. The Digital Analogs Knowledge System. <http://online.creservoirs.com/ccrl/jsp/login.jsp>.
- Chen, C.C., Ji, G.D., Wang, H.G., et al., 2022a. Geology-engineering integration to improve drilling speed and safety in ultra-deep clastic reservoirs of the Qiu-litage structural belt. *Adv. Geo-Energy Res.* 6 (4), 347. <https://doi.org/10.46690/ager.2022.04.09>.
- Chen, J., Lan, H., Macciotta, R., et al., 2018. Anisotropy rather than transverse isotropy in Longmaxi shale and the potential role of tectonic stress. *Eng. Geol.* 247, 38–47. <https://doi.org/10.1016/j.enggeo.2018.10.018>.
- Chen, J.P., Liang, D.G., Zhang, S.C., et al., 2012. Evaluation criterion and methods of the hydrocarbon generation potential for China's Paleozoic marine source rocks. *Acta Geol. Sin.* 86 (7), 1132–1142. <https://doi.org/10.3969/j.issn.0001-5717.2012.07.009> (in Chinese).
- Chen, J.Q., Zhang, X.G., Chen, Z.H., et al., 2021. Hydrocarbon expulsion evaluation based on pyrolysis Rock-Eval data: implications for Ordovician carbonates exploration in the Tabei Uplift. *Ar. J. Pet. Sci. Eng.* 196, 107614. <https://doi.org/10.1016/j.petrol.2020.107614>.
- Chen, X., Fan, J.X., Chen, Q., et al., 2014. Toward a stepwise Kwangsi Orogeny. *Sci. China Earth Sci.* 57 (3), 379–387. <https://doi.org/10.1007/s11430-013-4815-y>.
- Chen, Z.H., Jiang, C.Q., 2015. A data driven model for studying kerogen kinetics with application examples from Canadian sedimentary basins. *Mar. Petrol. Geol.* 67, 795–803. <https://doi.org/10.1016/j.marpetgeo.2015.07.004>.
- Chen, Z.H., Jiang, C.Q., Lavoie, D., et al., 2016. Model-assisted Rock-Eval data interpretation for source rock evaluation: examples from producing and potential shale gas resource plays. *Int. J. Coal Geol.* 165, 290–302. <https://doi.org/10.1016/j.coal.2016.08.026>.
- Chen, Z.H., Qiao, R.Z., Li, C.Y., et al., 2022b. Hydrocarbon generation potential and model of the deep lacustrine source rocks in the Dongying Depression, Bohai Bay Basin. *Mar. Petrol. Geol.* 140, 105656. <https://doi.org/10.1016/j.marpetgeo.2022.105656>.
- Cichon-Pupienis, A., Littke, R., Lazauskienė, J., et al., 2021. Geochemical and sedimentary facies study-Implication for driving mechanisms of organic matter enrichment in the lower Silurian fine-grained mudstones in the Baltic Basin (W Lithuania). *Int. J. Coal Geol.* 244, 103815. <https://doi.org/10.1016/j.coal.2021.103815>.
- Epelle, E.L., Gerogiorgis, D.I., 2020. A review of technological advances and open challenges for oil and gas drilling systems engineering. *AIChE J.* 66 (4), e16842. <https://doi.org/10.1002/aic.16842>.
- Espitalié, J., Marquis, F., Sage, L., et al., 1987. Géochimie organique du bassin de Paris. *Rev. Inst. Fr. Pét.* 42 (3), 271–302. <https://doi.org/10.2516/ogst:1987017>.
- Fang, R.H., L, M.J., Lü, H.T., et al., 2017. Oil charging history and pathways of the Ordovician carbonate reservoir in the Tuoputai region, Tarim Basin, NW China. *Petrol. Sci.* 14 (4), 662–675. <https://doi.org/10.1007/s12182-017-0196-8>.
- Gao, H., Li, H.Z., 2015. Determination of movable fluid percentage and movable fluid porosity in ultra-low permeability sandstone using nuclear magnetic resonance (NMR) technique. *J. Pet. Sci. Eng.* 133, 258–267. <https://doi.org/10.1016/j.petrol.2015.06.017>.
- Geng, Z., Wang, Y.F., 2020. Physics-guided deep learning for predicting geological drilling risk of wellbore instability using seismic attributes data. *Eng. Geol.* 279, 105857. <https://doi.org/10.1016/j.enggeo.2020.105857>.
- Guo, X.S., Hu, D.F., Li, Y.P., et al., 2019. Theoretical progress and key technologies of onshore ultra-deep oil/gas exploration. *Engineering* 5 (3), 458–470. <https://doi.org/10.1016/j.eng.2019.01.012>.
- Hanson, A.D., Ritts, B.D., Moldowan, J.M., 2007. Organic geochemistry of oil and source rock strata of the Ordos Basin, north-central China. *AAPG (Am. Assoc. Pet. Geol.) Bull.* 91 (9), 1273–1293. <https://doi.org/10.1306/05040704131>.
- Hao, F., Guo, T.L., Zhu, Y.M., et al., 2008. Evidence for multiple stages of oil cracking and thermochemical sulfate reduction in the Puguang gas field, Sichuan Basin, China. *AAPG (Am. Assoc. Pet. Geol.) Bull.* 92 (5), 611–637. <https://doi.org/10.1306/01210807090>.
- Hu, T., Pang, X.Q., Jiang, F.J., et al., 2021. Movable oil content evaluation of lacustrine organic-rich shales: methods and a novel quantitative evaluation model. *Earth Sci. Rev.* 214, 103545. <https://doi.org/10.1016/j.earscirev.2021.103545>.
- Hu, W., Scaringi, G., Xu, Q., et al., 2018. Suction and rate-dependent behaviour of a shear-zone soil from a landslide in a gently-inclined mudstone-sandstone sequence in the Sichuan basin. *China. Eng. Geol.* 237, 1–11. <https://doi.org/10.1016/j.enggeo.2018.02.005>.
- Hu, Z., Klaver, J., Schmatz, J., et al., 2020. Stress sensitivity of porosity and permeability of Cobourg limestone. *Eng. Geol.* 273, 105632. <https://doi.org/10.1016/j.enggeo.2020.105632> Get rights and content.
- Jacob, H., 1985. Disperse solid bitumens as an indicator for migration and maturity in prospecting for oil and gas: erdol und Kohle. *Erdgas, Petrochem.* 38 (8), 365–392.
- Jarvie, D.M., Hill, R.J., Ruble, T.E., et al., 2007. Unconventional shale-gas systems: the Mississippian Barnett Shale of north-central Texas as one model for thermogenic shale-gas assessment. *AAPG (Am. Assoc. Pet. Geol.) Bull.* 91 (4), 475–499. <https://doi.org/10.1306/12190606068>.
- Jiang, F.J., Pang, X.Q., Bai, J., et al., 2016. Comprehensive assessment of source rocks in the Bohai Sea area, eastern China. *AAPG (Am. Assoc. Pet. Geol.) Bull.* 100 (6), 969–1002. <https://doi.org/10.1306/02101613092>.
- Katz, B.J., Dittmar, E.I., Ehret, G.E., 2000. A geochemical review of carbonate source rocks in Italy. *J. Petrol. Geol.* 23 (4), 399–424. <https://doi.org/10.1111/j.1747-5457.2000.tb00494.x>.
- Klemme, H.D., Ulmishek, G.F., 1991. Effective petroleum source rocks of the world:

- stratigraphic distribution and controlling depositional factors. *AAPG (Am. Assoc. Pet. Geol.) Bull.* 75 (12), 1809–1851. <https://doi.org/10.1306/OC9B2A47-1710-11D7-8645000102C1865D>.
- Li, C.R., Pang, X.Q., Ma, X.H., et al., 2021. Hydrocarbon generation and expulsion characteristics of the Lower Cambrian Qiongzhusi shale in the Sichuan Basin, Central China: implications for conventional and unconventional natural gas resource potential. *J. Pet. Sci. Eng.* 204, 108610. <https://doi.org/10.1016/j.petrol.2021.108610>.
- Li, Q.Q., Li, B., Mei, W.H., et al., 2022. Genesis and sources of natural gas in fold-and-thrust belt: the Middle Permian in the NW Sichuan Basin. *Mar. Petrol. Geol.* 140, 105638. <https://doi.org/10.1016/j.marpetgeo.2022.105638>.
- Liu, B., Wang, H.L., Fu, X.F., et al., 2019. Lithofacies and depositional setting of a highly prospective lacustrine shale oil succession from the Upper Cretaceous Qingshankou Formation in the Gulong sag, northern Songliao Basin, northeast China. *AAPG (Am. Assoc. Pet. Geol.) Bull.* 103 (2), 405–432. <https://doi.org/10.1306/08031817416>.
- Liu, D., Li, J., Xie, Z.Y., 2014. Origin and significance of Sinian original and coexist bitumen of central Sichuan Basin. *Petroleum Geology&Experiment* 36 (2), 218–223. <https://doi.org/10.11781/sydz201402218> (in Chinese).
- Liu, D., Xie, Z.Y., Li, J., et al., 2013. The inorganic microelement characteristics and hydrocarbon potential prediction of algal dolomite in Dengying Formation from Sichuan Basin. *Sci. Technol. Eng.* 13 (10), 2791–2798. <https://doi.org/10.3969/j.issn.1671-1815.2013.10.034> (in Chinese).
- Liu, J.P., Zhang, X.F., Zhang, W.C., et al., 2022a. Carbon nanotube enhanced water-based drilling fluid for high temperature and high salinity deep resource development. *Petrol. Sci.* 19 (2), 916–926. <https://doi.org/10.1016/j.petsci.2021.09.045>.
- Liu, S.G., Zhang, Z.J., Huang, W.M., et al., 2010. Formation and destruction processes of upper Sinian oil-gas pools in the Dingshan-Lintan structural belt, southeast Sichuan Basin, China. *Petrol. Sci.* 7 (3), 289–301. <https://doi.org/10.1007/s12182-010-0071-3>.
- Liu, W.H., 2019. Advances in oil and gas geology of the early Paleozoic marine carbonate strata in China. *Bull. Mineral Petrol. Geochem.* 38 (5), 10. <https://doi.org/10.19658/j.issn.1007-2802.2019.38.131> (in Chinese).
- Liu, Y.C., Liu, B., Fu, J., et al., 2022b. Surface heat flow, deep formation temperature, and lithospheric thickness of the different tectonic units in Tarim Basin, Western China. *Lithosphere* 2022 (1), 3873682. <https://doi.org/10.2113/2022/3873682>.
- Liu, Y.C., Liu, B., Cheng, L.J., et al., 2021. Modeling of tectonic-thermal evolution of cretaceous qingshankou shale in the changling sag, southern Songliao Basin, NE China. *Front. Earth Sci.* 9, 694906. <https://doi.org/10.3389/feart.2021.694906>.
- Ma, X.H., Yang, Y., Wen, L., et al., 2019. Distribution and exploration direction of medium- and large-sized marine carbonate gas fields in Sichuan Basin, SW China. *Petrol. Explor. Dev.* 46 (1), 3–17. [https://doi.org/10.1016/S1876-3804\(19\)30001-1](https://doi.org/10.1016/S1876-3804(19)30001-1).
- Ma, Y.L., Li, M.W., Cai, X.Y., et al., 2020. Mechanisms and exploitation of deep marine petroleum accumulations in China: advances, technological bottlenecks and basic scientific problems. *Oil Gas Geol.* 41 (4), 655–672. <https://doi.org/10.11743/ogg20200401>.
- Makeen, Y.M., Hakimi, M.H., Abdullah, W.H., 2015. The origin, type and preservation of organic matter of the Barremian-Aptian organic-rich shales in the Muglad Basin, Southern Sudan, and their relation to paleoenvironmental and paleoclimate conditions. *Mar. Petrol. Geol.* 65, 187–197. <https://doi.org/10.1016/j.marpetgeo.2015.03.003>.
- Pang, B., Chen, J.Q., Pang, X.Q., et al., 2022. Driving forces and their relative contributions to hydrocarbon expulsion from deep source rocks: a case of the Cambrian source rocks in the Tarim Basin. *Petrol. Sci.* <https://doi.org/10.1016/j.petsci.2022.08.011>.
- Pang, X.Q., Jia, C.Z., Zhang, K., et al., 2020. The dead line for oil and gas and implication for fossil resource prediction. *Earth Syst. Sci. Data* 12 (1), 577–590. <https://doi.org/10.5194/essd-12-577-2020>.
- Pang, X.Q., Li, M.W., Li, S.M., 2005. Geochemistry of petroleum systems in the Niuzhuang South Slope of Bohai Bay Basin: Part 3. Estimating hydrocarbon expulsion from the Shahejie formation. *Org. Geochem.* 36 (4), 497–510. <https://doi.org/10.1016/j.orggeochem.2004.12.001>.
- Peng, J.W., Pang, X.Q., Shi, H.S., et al., 2016. Hydrocarbon generation and expulsion characteristics of Eocene source rocks in the Huilu area, northern Pearl River Mouth basin, South China Sea: implications for tight oil potential. *Mar. Petrol. Geol.* 72, 463–487. <https://doi.org/10.1016/j.marpetgeo.2016.02.006>.
- Peters, K.E., 1986. Guidelines for evaluating petroleum source rock using programmed pyrolysis. *AAPG (Am. Assoc. Pet. Geol.) Bull.* 70 (3), 318–329. <https://doi.org/10.1306/94885688-1704-11D7-8645000102C1865D>.
- Peters, K.E., Burnham, A.K., Walters, C.C., 2015. Petroleum generation kinetics: single versus multiple heating-ramp open-system pyrolysis. *AAPG (Am. Assoc. Pet. Geol.) Bull.* 99 (4), 591–616. <https://doi.org/10.1306/11141414080>.
- Qiu, N.S., Chang, J., Zuo, Y.H., et al., 2012. Thermal evolution and maturation of lower Paleozoic source rocks in the Tarim Basin, northwest China. *AAPG (Am. Assoc. Pet. Geol.) Bull.* 96 (5), 789–821. <https://doi.org/10.1306/09071111029>.
- Rippen, D., Littke, R., Bruns, B., et al., 2013. Organic geochemistry and petrography of Lower Cretaceous Wealden black shales of the Lower Saxony Basin: the transition from lacustrine oil shales to gas shales. *Org. Geochem.* 63, 18–36. <https://doi.org/10.1016/j.orggeochem.2013.07.013>.
- Shi, C.H., Cao, J., Selby, D., et al., 2020. Hydrocarbon evolution of the over-mature Sinian Dengying reservoir of the Neoproterozoic Sichuan Basin, China: insights from Re-Os geochronology. *Mar. Petrol. Geol.* 122, 104726. <https://doi.org/10.1016/j.marpetgeo.2020.104726>.
- Shi, C.H., Cao, J., Tan, X.C., et al., 2018. Hydrocarbon generation capability of Sinian-Lower Cambrian shale, mudstone, and carbonate rocks in the Sichuan Basin, southwestern China: implications for contributions to the giant Sinian Dengying natural gas accumulation. *AAPG (Am. Assoc. Pet. Geol.) Bull.* 102 (5), 817–853. <https://doi.org/10.1306/071117147417019>.
- Sun, X.L., Turczyn, A.V., 2014. Significant contribution of authigenic carbonate to marine carbon burial. *Nat. Geosci.* 7 (3), 201–204. <https://doi.org/10.1038/NNGEO2070>.
- Theloy, C., Sonnenberg, S.A., 2013. Integrating geology and engineering: implications for production in the Bakken Play. In: *Williston Basin/SPE/AAPG/SEG Unconventional Resources Technology Conference*. OnePetro. <https://doi.org/10.1190/urtec2013-100>.
- Thompson, C.L., Dembicki Jr., H., 1986. Optical characteristics of amorphous kerogens and the hydrocarbon-generating potential of source rocks. *Int. J. Coal Geol.* 6 (3), 229–249. [https://doi.org/10.1016/0166-5162\(86\)90003-0](https://doi.org/10.1016/0166-5162(86)90003-0).
- USGS, 2009. *Oil and Gas, USA* <http://energy.usgs.gov/oilgas.html>.
- Varma, A.K., Hazra, B., Mendhe, V.A., et al., 2015. Assessment of organic richness and hydrocarbon generation potential of Raniganj basin shales, West Bengal, India. *Mar. Petrol. Geol.* 59, 480–490. <https://doi.org/10.1016/j.marpetgeo.2014.10.003>.
- Wang, E.Z., Liu, G.Y., Pang, X.Q., et al., 2020b. An improved hydrocarbon generation potential method for quantifying hydrocarbon generation and expulsion characteristics with application example of Paleogene Shahejie Formation, Nanpu Sag, Bohai Bay Basin. *Mar. Petrol. Geol.* 112, 104106. <https://doi.org/10.1016/j.marpetgeo.2019.104106>.
- Wang, M., Li, M., Li, J.B., et al., 2022. The key parameter of shale oil resource evaluation: oil content. *Petrol. Sci.* 19 (4), 1443–1459. <https://doi.org/10.1016/j.petsci.2022.03.006>.
- Wang, W.Y., Pang, X.Q., Chen, Z.X., et al., 2019. Quantitative prediction of oil and gas prospects of the Sinian-lower Paleozoic in the Sichuan Basin in central China. *Energy* 174, 861–872. <https://doi.org/10.1016/j.energy.2019.03.018>.
- Wang, W.Y., Pang, X.Q., Chen, Z.X., et al., 2020a. Improved methods for determining effective sandstone reservoirs and evaluating hydrocarbon enrichment in petroliferous basins. *Appl. Energy* 261, 114457. <https://doi.org/10.1016/j.apenergy.2019.114457>.
- Wang, W.Y., Pang, X.Q., Chen, Z.X., et al., 2021. Quantitative evaluation of transport efficiency of fault-reservoir composite migration pathway systems in carbonate petroliferous basins. *Energy* 222, 119983. <https://doi.org/10.1016/j.energy.2021.119983>.
- Wang, Z.C., Jiang, H., Wang, T.S., 2014. Paleo-geomorphology formed during Tongwan tectonization in Sichuan Basin and its significance for hydrocarbon accumulation. *Petrol. Explor. Dev.* 41 (3), 338–345. [https://doi.org/10.1016/S1876-3804\(14\)60038-0](https://doi.org/10.1016/S1876-3804(14)60038-0).
- Wei, G.Q., Yang, W., Liu, M.C., et al., 2020. Distribution rules, main controlling factors and exploration directions of giant gas fields in the Sichuan Basin. *Nat. Gas. Ind. B* 7 (1), 1–12. <https://doi.org/10.1016/j.ngib.2020.01.001>.
- Wu, Z.Y., Zhao, X.Z., Pu, X.G., et al., 2022. Petroleum resource potential evaluation using insights based on hydrocarbon generation, expulsion, and retention capabilities: A case study targeting the Paleogene Es1 formation, Qikou Sag. *J. Pet. Sci. Eng.* 208, 109667. <https://doi.org/10.1016/j.petrol.2021.109667>.
- Xia, L.W., Cao, J., Wang, M., et al., 2019. A review of carbonates as hydrocarbon source rocks: basic geochemistry and oil-gas generation. *Petrol. Sci.* 16 (4), 713–728. <https://doi.org/10.1007/s12182-019-0343-5>.
- Xu, H.L., Wei, G.Q., Jia, C.Z., et al., 2012. Tectonic evolution of the Leshan-Longnüsi paleo-uplift and its control on gas accumulation in the Sinian strata. *Petrol. Explor. Dev.* 39 (4), 436–446. [https://doi.org/10.1016/S1876-3804\(12\)60060-3](https://doi.org/10.1016/S1876-3804(12)60060-3).
- Yan, X.P., Kang, Y.L., You, L.J., et al., 2019. Drill-in fluid loss mechanisms in brittle gas shale: a case study in the Longmaxi Formation, Sichuan Basin, China. *J. Pet. Sci. Eng.* 174, 394–405. <https://doi.org/10.1016/j.petrol.2018.11.026>.
- Yang, S.Y., Horsfield, B., 2020. Critical review of the uncertainty of Tmax in revealing the thermal maturity of organic matter in sedimentary rocks. *Int. J. Coal Geol.* 225, 103500. <https://doi.org/10.1016/j.coal.2020.103500>.
- Yao, L.P., Zhong, N.N., Khan, I., et al., 2021. Comparison of in-source solid bitumen with migrated solid bitumen from Ediacaran-Cambrian rocks in the Upper Yangtze region, China. *Int. J. Coal Geol.* 240, 103748. <https://doi.org/10.1016/j.coal.2021.103748>.
- Zhang, D.W., 2022. Development prospect of natural gas industry in the Sichuan Basin in the next decade. *Nat. Gas. Ind. B* 9 (2), 119–131. <https://doi.org/10.1016/j.ngib.2021.08.025>.
- Zhang, S.C., Shuai, Y.H., 2015. Geochemistry and distribution of biogenic gas in

- China. Bull. Can. Petrol. Geol. 63 (1), 53–65. <https://doi.org/10.2113/gscpgbull.63.1.53>.
- Zhou, J., Pang, X.Q., 2002. A method for calculating the quantity of petroleum generation and expulsion. Petrol. Explor. Dev. 29, 24–27 doi:1000-0747(2002)01-0024-04 (in Chinese).
- Zhou, J.G., Xu, C.C., Yao, G.S., et al., 2015. Genesis and evolution of lower cambrian longwangmiao formation reservoirs, Sichuan Basin, SW China. Petrol. Explor. Dev. 42 (2), 175–184. [https://doi.org/10.1016/S1876-3804\(15\)30004-5](https://doi.org/10.1016/S1876-3804(15)30004-5).
- Zhu, L.Q., Liu, G.D., Song, Z.Z., et al., 2022. Reservoir solid bitumen-source rock correlation using the trace and rare earth elements-implications for identifying the natural gas source of the Ediacaran-Lower Cambrian reservoirs, central Sichuan Basin. Mar. Petrol. Geol. 137, 105499. <https://doi.org/10.1016/j.marpetgeo.2021.105499>.
- Zou, C.N., Du, J.H., Xu, C.C., et al., 2014b. Formation, distribution, resource potential, and discovery of Sinian-Cambrian giant gas field, Sichuan Basin, SW China. Petrol. Explor. Dev. 41 (3), 306–325. [https://doi.org/10.1016/S1876-3804\(14\)60036-7](https://doi.org/10.1016/S1876-3804(14)60036-7).
- Zou, C.N., Guo, J.L., Jia, A.L., et al., 2020. Connotation of scientific development for giant gas fields in China. Nat. Gas. Ind. B. 40 (3), 1–12. <https://doi.org/10.1016/j.ngib.2020.09.011>.
- Zou, C.N., Wei, G.Q., Xu, C.C., et al., 2014a. Geochemistry of the Sinian-cambrian gas system in the Sichuan Basin. China. Org. Geochem. 74, 13–21. <https://doi.org/10.1016/j.orggeochem.2014.03.004>.
- Zou, C.N., Zhu, R.K., Wu, S.T., et al., 2012. Types, characteristics, genesis and prospects of conventional and unconventional hydrocarbon accumulations: taking tight oil and tight gas in China as an instance. Acta Petrol. Sin. 33 (2), 173–187 doi:0253-2697(2012)02-0173-15 (in Chinese).